DIETZ'S THEORY EXTENDED TO FRONTAL ADVANCE AROUND AN INJECTION WELL

Arild Eldøy, Statoil

Ole Nygård, Statoil

Svein M. Skjæveland, Rogaland Regional College

Beginning of the text, 1st column, 1st lign

ABSTRACT

During water injection in a horizontal formation, gravity underride of water may occur even close to the wellbore, if the mobility ratio is adverse. A water tongue will develop and effect the interpretation of pressure falloff tests and also the total reservoir sweep efficiency. In this paper a simpel analytical expression is developed for prediction of frontal advance of water from an injection well as a function of time, when gravity effects are important. Isothermal flow is assumed, and the development follows closely that of Dietz for a linear system. The assumptions made in establishing the differential equation are tested by the use of a numerical simulator, and the approximations made in deriving the first and second order analytical solutions are tested by a direct numerical solution of the differential equation. Through a field example from a falloff test, possible applications of the theory are demonstrated. The theory should also be applicable for predicting frontal advance of gas from injection wells, if gas dissolution in the oil and compressiblity effects are neglected. The present paper, however, concentrates on water injection.

RESUME

Lorsque l'on injecte de l'eau dans une formation horizontale, une instabilité gravitaire de l'eau peut survenir même près du puits si le rapport des mobilités est défavorable. Une langue d'eau se développera et aura une influence sur les interpretations des tests de chute de pression (fall-off), et aussi sur l'efficacité de balayage du gisement tout entier. Cet article développe une expression analytique simple pour predire l'avance du front d'eau à partir d'un puits d'injection en fonction du temps, quand les forces de gravité sont importantes. L'écoulement est supposé isotherme et le développement suit étroitement celui de Dietz pour un système lineaire. Les hypothèses faites pour établir l'équation differentielle sont testées au moyen d'un simulateur numérique et les approximations faites en dérivant au premier et second ordre les solutions analytiques sont testées par une solution numérique directe de l'équation differentielle. Dans un exemple de champ, à partir d'un test de chute de pression, des applications possibles de la théorie sont demontrées. Cette théorie devrait être aussi applicable pour prédire l'avance frontale du gaz à partir des puits d'injection, si la dissolution du gaz dans l'huile et les effets de compressibilité sont négligeables. Cependant, cet article s'intéresse plus particulièrement à l'injection d'eau.

To be continued 2nd column, 1st lign

1. INTRODUCTION

Full field waterflooding is planned for several of the oil fields on the Norwegian continental shelf. Exploratory wells are therefore tested for injectivity, and injectors will be tested during field operation. The amount of pressure falloff test data will increase. If methods for detailed interpretation had been available, these tests could give information about frontal advance, residual oil saturation and verify the flow characteristics of the virgin for-

mation. Even if a rather simplistic model of the reservoir is assumed, it is, however, fairly difficult to interpret a falloff test.

Merrill et al [1] assumed a composite system with piston-like displacement and claimed that proper analysis of falloff tests in waterflood systems that form two contrasting fluid zones can give information as to (a) mobilities on both sides of the front, (b) saturations on both sides of the front, and (c) distance to the front. Sosa et al [2] demonstrated that, except for a very low mobility ratio, the falloff pressure curve will reflect a saturation distribution behind the front, i.e. the assumption of piston-like diplacement is invalid. Several authors, e.g. Benson and Bodvarsson [3], Brown et al [4], have pointed out that nonisothermal effects also have to be considered when interpreting a falloff test following cold water injection into a hot reservoir. If the early and late falloff pressure data can be interpreted to give the mobilities of the water zone close to the wellbore and that of the virgin formation, respectively, with a transition period in between, the inclusion of temperature and saturation distribution effects will expand the transition period.

In the studies mentioned, gravity effects have been neglected. If these are important, interpretation of falloff tests will be even more complicated since a pronounced underriding water tongue also will extend the transition period between the responses from the two zones.

The objective of this study is to evaluate the isolated effect of the gravity term on fluid distribution during isothermal, piston-like displacement from a water injector. A simple analytical expression is derived to monitor the water front as a function of time. The possible importance of the effect is demonstrated in connection with an actual field test. No effort has been made to interpret the test with all the complicating factors included. The result can be used to quantify the importance of gravity effects in a falloff test, and also the near-well, vertical sweep efficiency.

2. THEORY

The theoretical development follows closely that of Dietz [5], who presented the classical theory for gravity-influenced water displacement in a linear system. The initial steps also resemble those of van Lookeren [6], who, based on Dietz's theory, developed an expression for steam-zone development around an injection well.

2.1 Assumptions

The basic assumptions are as follows:

1) The oil reservoir is horizontal with constant thickness, uniform porosity, constant permeability and has infinite radial extent and irreducible water saturation.

2) The well is vertical and perforated over the reservoir height.

3) Water is injected at a constant reservoir rate q and compressibility effects of water, oil and formation can be neglected.

4) The microscopic water displacement is piston-like with a saturation step change in that part of the cross-section which has been contacted by water.

5) Thermal effects are neglected.

6) Capillary effects are neglected.

7) Vertical gravity equilibrium exists within both the oil and water column. This assumption implies that all flow takes place in the horizontal direction only.

8) The mobility ratio $M > 1$.

2.2 Derivation of differential equation

Figure 1 is a sketch of the water-oil interface, $y(r,t)$, after the gravity forces have destabilized the initially vertical front and a viscous finger in the form of a gravity tongue has developed at the bottom of the reservoir.

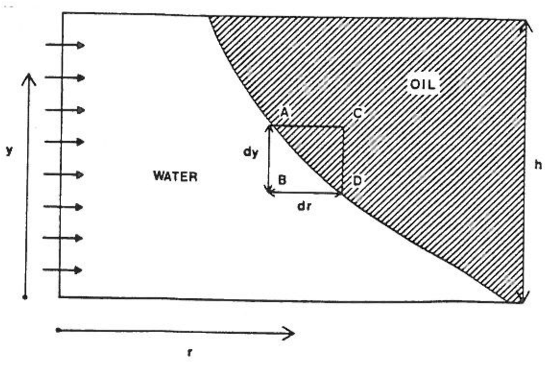

FIGURE 1 Sketch of the water-oil interface after a gravity tongue has developed.

DIETZ'S THEORY EXTENDED TO FRONTAL ADVANCE AROUND AN INJECTION WELL

By using the vertical equilibrium condition on the infinitesimal rectangle ABCD we get the following relation between the radial pressure gradients at the interface:

$$\frac{\partial P_w}{\partial r} - \frac{\partial P_o}{\partial r} = \Delta\rho g \frac{\partial y}{\partial r} . \qquad (1)$$

From Darcy's law:

$$q_o = -2\pi(h-y)r\lambda_o \frac{\partial P_o}{\partial r} \qquad (2)$$

$$q_w = -2\pi y r \lambda_w \frac{\partial P_w}{\partial r} , \qquad (3)$$

since, by assumption of vertical equilibrium within each phase, the pressure gradients in radial direction are constant, for a given radius r, over the heights y and h-y for water and oil respectively.

Total continuity of the liquids and continuity of the water phase give:

$$q_o + q_w = q , \qquad (4)$$

$$\frac{\partial q_w}{\partial r} = -2\pi r \phi S \frac{\partial y}{\partial t} , \qquad (5)$$

where S denotes the step change in water saturation. The last equation expresses the radial change of the water rate in terms of the change of the interface with time.

From Eqs.1-3, eliminating the pressure gradients, we get

$$2\pi r \Delta\rho g \lambda_o \frac{\partial y}{\partial r} = \frac{1}{h-y} q - \left(\frac{a}{y} + \frac{1}{h-y}\right) q_w , \qquad (6)$$

where a = 1/M. Differentiation of this equation with respect to r gives

$$2\pi\Delta\rho g\lambda_o \frac{\partial^2 y}{\partial r^2} = -\frac{1}{r^2}\left[\frac{q}{h-y} - \left(\frac{a}{y} + \frac{1}{h-y}\right) q_w\right] +$$

$$\frac{1}{r}\left[\frac{q}{(h-y)^2}\frac{\partial y}{\partial r} + \left(\frac{a}{y^2} - \frac{1}{(h-y)^2}\right) q_w \frac{\partial y}{\partial r} -\right.$$

$$\left.\left(\frac{a}{y} + \frac{1}{h-y}\right)\frac{\partial q_w}{\partial r}\right]. \qquad (7)$$

Into this equation is now substituted the expression for the rate q_w from Eq. 6 and its derivative from Eq. 5. We also substitute the identity

$$\frac{\partial y}{\partial t} = -\frac{\partial y}{\partial r}\frac{\partial r}{\partial t} ,$$

and after rearranging the terms, we get the following equation

$$F_1 \frac{\partial^2 y}{\partial r^2} + \frac{F_1+F_2}{r}\frac{\partial y}{\partial r} + F_3\left(\frac{\partial y}{\partial r}\right)^2 =$$

$$-F_4 \frac{\partial y}{\partial r}\frac{\partial r}{\partial t} , \qquad (8)$$

with

$$F_1 = 2\pi\Delta\rho g\lambda_o (h-y)y$$

$$F_2 = -\frac{qah}{a(h-y)+y}$$

$$F_3 = 2\pi\Delta\rho g\lambda_o \frac{a(h-y)^2 - y^2}{a(h-y)+y}$$

$$F_4 = 2\pi\phi S\,[a(h-y) + y], \qquad (9)$$

and with the boundary condition that the front starts out vertically at t=0, r=0 (or $r=r_w$).

2.3 First order solution

We try to solve Eq.8 by a perturbative approach. To the first order we neglect the gravity terms and then introduce them in the second order solution as a perturbation. By setting $\Delta\rho=0$, we retain only the coefficients F_2 and F_4. The procedure is reasonable if the second order terms $\partial^2 y/\partial r^2$ and $(\partial y/\partial r)^2$ have the same type of r-singularity, $1/r(\partial y/\partial r)$, as that of the retained term. This will be demonstrated below. We are then left with

$$\frac{F_2}{r}\frac{\partial y}{\partial r} = -F_4 \frac{\partial y}{\partial r}\frac{\partial r}{\partial t} . \qquad (10)$$

Eliminating $\partial y/\partial r$ and defining $C_1 = -F_2/F_4$ we have

$$r\frac{\partial r}{\partial t} = C_1(y), \qquad (11)$$

with the solution

$$r^2 = 2C_1 t + c(y), \qquad (12)$$

where c(y) is an integration constant. Using the boundary condition that $r=r_w$ for all y when t=0, we have the first order solution

$$r^2 = 2C_1 t + r_w^2 , \qquad (13)$$

$$C_1 = \frac{q}{2\pi\phi S} \; \frac{ah}{[a(h-y)+y]^2} .$$

2.4 Second order solution

We now use the first order solution, Eq. 13, to evaluate the first and second derivative of y with respect to r in order to introduce these terms into the complete equation, Eq.8. For simplicity we set $r_w=0$. Differentiation of Eq.13 with respect to r gives

$$2r = 2t \frac{\partial C_1}{\partial y} \frac{\partial y}{\partial r} .$$

After differentiation, substitution for t from Eq. 13 and rearrangement, we get

$$\frac{\partial y}{\partial r} = \frac{1}{r} \; \frac{a(h-y)+y}{a-1} . \qquad (14)$$

A second differentiation gives

$$\frac{\partial^2 y}{\partial r^2} = -\frac{2}{r} \frac{\partial y}{\partial r} . \qquad (15)$$

Inserting Eqs.14 and 15 into Eq.8, we arrive at the same type of equation as given in Eq.11 with the second order solution

$$r^2 = 2(C_1 + C_2 + C_3)\, t + r_w^2 , \qquad (16)$$

where

$$C_1 = \frac{q}{2\pi\phi S} \; \frac{ah}{[a(h-y)+y]^2} ,$$

$$C_2 = \frac{\Delta\varrho g\lambda_o}{\phi S} \; \frac{y(h-y)}{a(h-y)+y} ,$$

$$C_3 = \frac{\Delta\varrho g\lambda_o}{\phi S} \; \frac{a(h-y)^2 - y^2}{[a(h-y)+y](1-a)} .$$

2.5 Discussion

During water injection, the dimensionless injection rate q_D, defined by

$$q_D = \frac{q}{2\pi\Delta\varrho g\lambda_o h^2} , \qquad (17)$$

has to exceed a critical rate q_D^c if the water is to enter the formation over the total thickness h. The critical rate can be estimated from Eq.16 by requiring that the front at the top of the formation, y=h, remains at $r=r_w$ for all t. This gives

$$q_D^c = \frac{1}{a(1-a)} = \frac{M^2}{M-1} . \qquad (18)$$

If $q_D < q_D^c$, the water will enter only over a fraction of the height h. The height of highest entry can be estimated from Eq.16 by finding the value of y which renders the sum of the C's equal zero.

The rationale for the perturbative approach can be checked by comparing the magnitudes of the first and second order terms. The requirement is that $C_1 > C_2 + C_3$, directly from Eq.16, or, equivalently, from Eq.8 after insertion of first and second order derivatives. In Appendix A is shown that the first order solution is valid for $q_D \gg q_D^c$ and the second order solution for $q_D > q_D^c$, with the largest deviation occurring at the top of the formation.

From Eq.18 it is seen that the second order solution breaks down when a is close to 1. Then, from Eq.14, the front stays vertical.

The validity of the analytical, approximate solution is demonstrated below, where a direct numerical solution is performed based on the complete Eq.8.

The solution is, of course, hampered by the assumptions made in Sec. 2.1. We will here comment on a few of them.

- The addition of capillary pressure will cause a diffuse water-oil interface, probably retarding the advance of the water gravity tongue increasingly with radius, since the horizontal, viscous force decreases with 1/r, while the capillary-gravity forces are constant. The effect will depend on the ratio between the static gravity-capillary transition zone and the formation height, as discussed by Croes et al [7].

- According to the theory of Buckley and Leverett [8], the microscopic displacement is not in general of the complete step-saturation change but leaves a saturation distribution behind the front. This will cause some gravity segregation to take place in the water-invaded area, and also reduction in the water mobility behind the front. The last effect can be corrected for by using the water mobility at the average

saturation behind the front, as suggested by Craig [9].

- There are some arguments to substantiate assumption (7) of horizontal flow only. Neglecting friction losses in the well over the formation height, the water column in the well is always in gravity equilibrium, causing gravity equilibrium within the water tongue close to the well. The initial, vertical, gravity-unstable front at the sandface will cause the water to enter at the bottom of the formation, and with M>1, the viscous finger of the water will continue to grow below the oil zone. At distances far from the well, gravity equilibrium exists since the gravity gradient is constant, while the horizontal pressure gradient is proportional to 1/r. Below, we have given support to these arguments by simulating waterfloods with a numerical reservoir model for different ratios of vertical to horizontal permeability.

Although the theory is derived for a water-oil system, it should also be applicable to gas injection in an oil zone, as shown by Hawthorne [10] for a linear system.

3. NUMERICAL SOLUTION OF DIFFERENTIAL EQUATION

In this section is presented numerical solutions to the differential equation, Eq.8, in order to check the validity of the analytical solution procedure.

3.1 Numerical method

The partial differential equation, Eq.8, is reformulated to

$$\frac{\partial r}{\partial t} = -\frac{F_1}{F_4}\,\frac{\dfrac{\partial^2 y}{\partial r^2}}{\dfrac{\partial y}{\partial r}} - \frac{1}{r}\,\frac{F_2+F_1}{F_4} - \frac{F_3}{F_4}\,\frac{\partial y}{\partial r} \qquad (19)$$

The velocity of the front for a given y is $\partial r/\partial t$. A fixed grid is used in the y-direction. For each grid value of y, the F's are evaluated, being functions of y only. The first and second order derivatives on the left hand side of Eq.19 are approximated by a standard finite difference scheme. The scheme is explicit in the sense that derivatives at the old frontal positions are used to evaluate the new positions, except for the 1/r term. The value of r is approximated by the arithmetic average of old and new value. For a given timestep Δt, the change Δr i frontal position for a given y can then be calculated from the discrete version of Eq.19.

Initially the front is vertical and $\partial y/\partial r$ is undefined. For the first small timestep we therefore use the first order solution, Eq.13, and then Eq.19 for all consecutive timesteps.

A FORTRAN IV program was written to solve the problem. The program was extensively tested and discretization errors controlled by having a fine grid in the y-direction and using small timesteps. Also, the program makes a simple triangular integration on the front to calculate the volume of water behind the front. When compared with volume water injected, this gives a material balance check which was excellent for all cases investigated.

3.2 Examples

Example 1 is the base case from Appendix B. Figure 2 shows the frontal advance as a function of injection time. Plotted in the figure are the numerical and the first and second order analytical solutions.

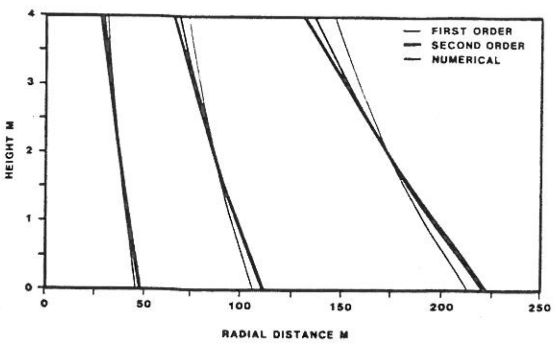

FIGURE 2 Development of front for base case. Numerical, 1 and 2 order analytical solutions. Fronts depicted at 46, 250 and 1000 hrs.

The front enters the total formation thickness, as could be expected since $q_D \gg q_D^c$, and gradually develops a gravity tongue. The second order solution is closest to the numerical solution with the largest difference at the top of the formation.

DIETZ'S THEORY EXTENDED TO FRONTAL ADVANCE AROUND AN INJECTION WELL

First column, first lign
To be continued. End column 1st lign

In example 2, Figure 3, we have increased the mobility ratio to M=10 by reducing the water viscosity. Then q_D^c=11.1, a factor 2 below q_D.

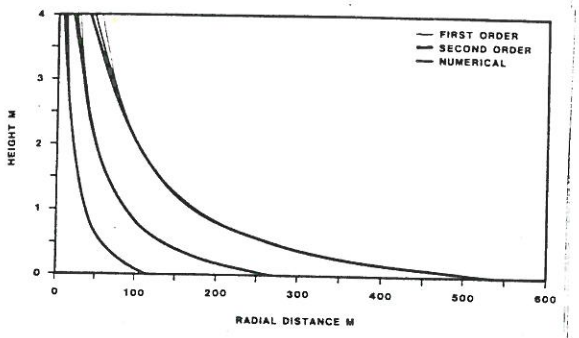

FIGURE 3 Development of front for base case with mobility ratio increased to M=10. Numerical, 1 and 2 order analytical solutions. Fronts depicted at 46, 250 and 1000 hrs.

As could be expected, the front barely enters the top of the formation and a severe water gravity tongue is seen.

4. SOLUTION BY NUMERICAL SIMULATOR

In this section we have compared the 2. order analytical solution with the results of a numerical reservoir simulator. Two cases have been treated to investigate the influence of the k_v/k_h ratio. In case 1, the base case from Appendix B is run with permeability ratios of 1. and 0.1. In case 2 the same runs are repeated with M=10, as in example 2, Sec. 3.

Due to numerical dispersion, the frontal position is not well defined from the numerical model. We have chosen to use the saturation at the front, as calculated from the Buckley-Leverett theory, to plot the frontal advance from the simulator results.

The relative permeability curves from Appendix B have been used in all the runs. The microscopic displacement efficiency is therefore not piston-like, as assumed in the theory, especially not at high values of the mobility ratio M. Gravity segregation will therefore occur behind the front, probably enhancing the growth of the viscous finger, as compared with the theory.

4.1 Numerical model

The numerical model is a three-phase, two-dimensional, implicit, finite difference model with simultaneous and direct solution of pressure and saturation changes, ref. [11]. The model was run in radial mode with a numerical grid as sketched in Figure 4.

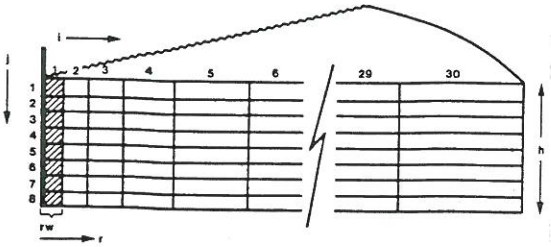

FIGURE 4 Sketch of the numerical grid

In case 1, the numerical grid is as sketched in Figure 4 with numerical layers of equal height. In case 2, the heights of the layers are smaller at the bottom in order to better define the thin gravity tongue. The first vertical column is part of the wellbore and is given a vertical and horizontal permeability of 10^9 Darcies to ensure an infinite conductivity well and correct distribution of water between the layers. The sum of r_w and the first blocklength equals the actual wellbore radius of 0.107m. The last vertical column is given a high porosity in order to artificially simulate an infinite reservoir. The timestep size was automatically controlled by a maximum prescribed saturation change of 0.05 or pressure change of 1034 kPa. Sensitivity to timestep and block sizes was not systematically investigated. Capillary pressure was set to zero in all runs.

4.2 Example runs, case 1

Two runs were made, all with data from the base case in Appendix B, except for the following changes:

Run 1: k_v/k_h=1.0 (as in base case).

Run 2: k_v/k_h=0.1

The fronts, at a water saturation of 0.46, are depicted in Figure 5 at various stages together with the frontal position from the second order analytical solution.

DIETZ'S THEORY EXTENDED TO FRONTAL ADVANCE AROUND AN INJECTION WELL

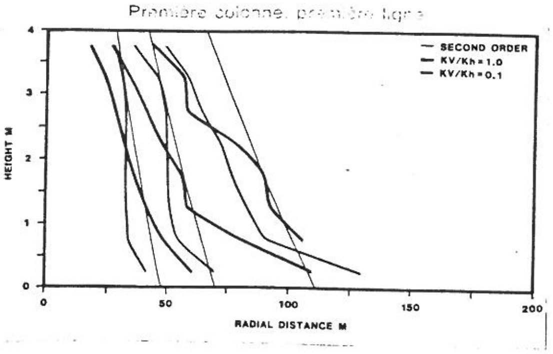

FIGURE 5 Frontal development for the two runs in case 1 together with second order analytical solution. Fronts depicted at 46, 100 and 250 hrs.

On an average, the analytical solution is to the right of the two simulator results, for all three stages of frontal development. This is probably caused by numerical dispersion. The simulator fronts are depicted at the Buckley-Leverett breakthrough saturation of 0.46, but the water has penetrated farther into the reservoir in the simulation runs. If numerical dispersion had been suppressed, the simulator fronts would have moved to the right, by volume balance.

The slope of the front for the low permeability-ratio run is initially steeper than that of the high permeability-ratio run. The slope from the analytical solution lies in between at 46 and 100 hrs., and is closest to the low permeability-ratio run at 250 hrs.

The slope of the high permeability-ratio run is lower than that of the analytical solution for all three stages, and the difference increases with time. The reason for this is probably gravity segregation behind the front in the simulator run. Movable water behind the front will segregate to the bottom of the formation and enhance the growth of the viscous finger. The average water saturation behind the front, at the bottom of the formation, will thus be higher than that calculated from the Buckley-Leverett theory, which is used in the analytical solution to determine the mobility ratio M.

4.3 Example runs, case 2

The same two simulation runs as in case 1 were repeated, but with a mobility ratio M=10, achieved by artificially reducing the water viscosity. The fronts are shown in Figure 6 after 46 hours of injection.

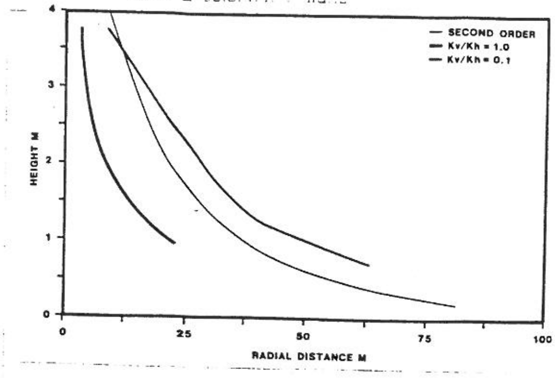

FIGURE 6 Frontal position for the two runs in case 2 together with the second order analytical solution. Fronts depicted at 46 hrs.

From a Buckley-Leverett calculation, the front saturation is 0.32 and the average water saturation behind the front is 0.34, which has been used to calculate M=10. The two fronts from the simulation runs have therefore been drawn at a water saturation of 0.32. They are terminated at a height of 1 m due to the limitations on the number of grid blocks available. To properly define the two fronts below 1 m, a finer grid in the r-direction would be required, in addition to the finer vertical grid used at the bottom of the formation.

Reduction of numerical dispersion would also in this case have shifted the two fronts from the simulation runs to the right in the figure.

The front for the high permeability-ratio run is farthest to the left in the figure because a higher degree of gravity segregation takes place behind the front.

5. DISCUSSION

With all the assumptions included in establishing the differential equation, Eq.8, we have demonstrated the validity of the analytical solution, Eq.16, for $q_D > q_D^c$. The numerical simulation results indicate that the theory may also be useful in predicting frontal advance if the assumptions of piston-like displacement and vertical equilibrium are removed. The simulation results in Figures 5 and 6 show reasonable good agreement with the theory. However, a more exhaustive numerical simulation study is required to delineate the general range of validity for the theory. The inclusion of capillary pressure would probably retard the growth of the gravity tongue. Also, the shape of the relative permeability curves will influence

DIETZ'S THEORY EXTENDED TO FRONTAL ADVANCE AROUND AN INJECTION WELL

the approximation of piston-like displacement.

In design and interpretation of a falloff test, the rather simple, analytical solution can be used to estimate the transition zone between the water-invaded part of the reservoir close to the wellbore and the uninvaded, virgin part of the formation. If the theory proves to have a fairly general validity, an estimation of the mobility ratio from the test could be possible.

6. CONCLUSIONS

Based on several assumptions, a simple analytical expression is derived for monotoring the frontal advance of water from an injection well.

A crital injection rate is suggested, below which the water will enter only over part of the formation height.

Simulation runs based on limited variations in input data indicate that all assumptions are not strictly necessary. The theory could be valid over a range of reservoir and injection conditions, but further investigations need to be done to verify this possibility.

The theory can also be applied to frontal advance from gas injectors if gas dissolution in oil is neglected.

The theory can be used to evaluate the near-well vertical sweep efficiency and to estimate the transition zone caused by gravity effects between waterflooded and virgin formation in a falloff test.

7. LIST OF SYMBOLS

All equations are written in SI-units as given below, not the preferred API Standard SI-units.

Symbol	Meaning	Units
a	inverse mobility ratio	
C	coefficients, Eqs. 13 and 16	
F	coefficients, Eq. 9	
g	9.80665, gravity constant	ms^{-2}
h	formation height	m
k_h	horizontal permeability	m^2
k_v	vertical permeability	m^2
k_{ro}	oil relative permeability	
k_{rw}	water relative permeability	
M	mobility ratio	
P_o	oil pressure	Pa
P_w	water pressure	Pa
P	Polynomial in Appendix A	
q	injection rate, res. cond.	m^3/s
q_o	oil rate, res. cond.	m^3/s
q_w	water rate, res. cond.	m^3/s
q_D	dimensionless rate	
q_D^c	dimensionless critical rate	
r	radius to front	m
r_D	dimensionless radius to front	
r_w	wellbore radius	m
S	$S_{oi}-S_{or}$, step saturation change	
S_o	oil saturation	
S_w	water saturation	
S_{oi}	initial oil saturation	
S_{or}	residual oil saturation	
t	time	s
t_D	dimensionless time	
y	height to front	m
Y	dimensionless height to front	
Y_m	local minimum position of P(Y)	
λ_o	$k_h k_{ro}/\mu_o$, horiz. oil mobility	$m^2/Pa\ s$
λ_w	$k_h k_{rw}/\mu_w$, horiz. wat. mobility	$m^2/Pa\ s$
μ_o	oil viscosity	Pa s
μ_w	water viscosity	Pa s
ϱ_o	oil density	$kg\ m^{-3}$
ϱ_w	water density	$kg\ m^{-3}$
$\Delta\varrho$	$\varrho_w - \varrho_o$	$kg\ m^{-3}$
ϕ	porosity	

8. REFERENCES

1. Merrill, L.S., Kazemi, H. and Gogarty, W.B.: "Pressure Falloff Analysis in Reservoirs with Fluid Banks," J. Pet. Tech. (July 1974) 809-818.

2. Sosa, A., Raghavan, R. and Limon, T.J.: "Effect of Relative Permeability and Mobility Ratio on Pressure Falloff Behavior," J. Pet. Tech. (June 1981) 1125-1135.

Recall of the title of the paper (in capital letters)
Rappel du titre de la communication (en lettres majuscules)

DIETZ'S THEORY EXTENDED TO FRONTAL ADVANCE AROUND AN INJECTION WELL

First column, first lign

To be continued 2nd column 1st lign

3. Benson, S.M. and Bodvarsson, G.S.: "Non-isothermal Effects during Injection and Falloff Tests," paper SPE 11137 presented at the 57th Annual Meeting, New Orleans, Sept.26-29,1982.

4. Brown, C.E., Christie, M.A. and Gatt, A.M.: "Reservoir Temperature Distribution around Injection Wells - Effect on EOR Schemes," paper presented at the 2nd European Symposium on Enhanced Oil Recovery, Paris,1982.

5. Dietz, D.N.: "A Theoretical Approach to the Problem of Encroaching and Bypassing Edge Water," Proc., Kon. Ned. Akad. Wetensch., Amsterdam (1953), B56, 83-92.

6. van Lookeren, J.: "Calculation Methods for Linear and Radial Steam Flow in Oil Reservoirs," Soc. Pet. Eng. J. (June 1983) 427-439.

7. Croes, G.A. and Schwarz, N.: "Dimensionally Scaled Experiments and the Theories on the Water-Drive Process," Trans., AIME(1955) 35-42.

8. Buckley, S.E. and Leverett, M.C.: "Mechanism of Fluid Displacement in Sands," Trans., AIME(1942) 107-116.

9. Craig, F.F.: The Reservoir Engineering Aspects of Waterflooding, Monograph Series, SPE, Dallas (1971) 3, Ch. 4.

10. Hawthorne, R.G.: "Two-Phase Flow in Two-Dimensional Systems - Effects of Rate, Viscosity and Density on Fluid Displacement in Porous Media," Trans. AIME(1960) 81-87.

11. "User's Manual for TODVARS," Rogaland Research Institute, 1984.

APPENDIX A - DISCUSSION OF SECOND ORDER CORRECTION TERM

We rewrite Eq.16 in dimensionless form with $Y=y/h$, and $r_w=0$ for simplicity:

$$r_D^2 = 2t_D \frac{a}{[a(1-Y)+Y]^2} [q_D - P(Y)] \qquad (A1)$$

where

$$P(Y) = -\frac{[Y(1-Y)(1-a)+a(1-Y)^2-Y^2][a(1-Y)+Y]}{a(1-a)}$$

$$= \frac{[Y(1-a)+a]^2(2Y-1)}{a(1-a)} .$$

The first order solution is valid if $q_D >> |P(Y)|$ on the interval $Y\varepsilon[0,1]$. By inspection of the third order polynomial $P(Y)$ and its first and second order derivatives, we find that it may have at most a local minimum at $Y_m=(1-2a)/(3-3a)$ on the interval. When $a>0.5$, the minimum is outside the interval and $P(Y)$ is monotonously increasing with Y. By comparing the absolute values of $P(0)$, $P(Y_m)$ and $P(1)$ we find that $\max|P(Y)| = P(1) = 1/[a(1-a)] = q_D^c$ for all $a<1$ and $Y\varepsilon[0,1]$. Therefore, the first order solution is valid for $q_D >> q_D^c$ and the second order solution is valid for $q_D > q_D^c$, i.e. if the water enters over the total formation thickness h. The deviation from the correct solution will be more pronounced at the top of the formation where $|P(Y)|$ has its maximum. The solutions are equal at $Y=0.5$.

APPENDIX B - BASE CASE

The base case is taken from an injectivity test in a highly permeable sandstone reservoir. All data are presented and used at reservoir temperature and pressure. Prior to injection, a drillstem test was performed to determine properties of the virgin formation.

DATA

Initial pressure: 31590 kPa

Saturation pressure: 21100 kPa

Oil viscosity: $1.2\ 10^{-3}$ Pa s

Oil density: 665.8 kg m^{-3}

Water viscosity: $0.4\ 10^{-3}$ Pa s

Water density: 1018.8 kg m^{-3}

Water injection rate: 0.0127 $m^3\ s^{-1}$

Porosity: 0.307

Initial water saturation: 0.28

Irreducible water saturation: 0.28

Horizontal permeability: $4.561\ 10^{-12}\ m^2$

Vertical permeability assumed equal to horizontal permeability in base case.

Formation height: 4.0 m

Wellbore radius: 0.107 m

Recall of the title of the paper in capital letters
Rappel du titre de la communication en lettres majuscules

DIETZ'S THEORY EXTENDED TO FRONTAL ADVANCE AROUND AN INJECTION WELL

First column, first ligh

To be continued, 2nd column, 1st ligh

Injection time for test: 46 hrs. In some of the examples 1000 hrs have been used for demonstration purposes.

Relative permeabilities:

S_w	k_{rw}	k_{ro}
0.06	0.00	1.00
0.10	0.00	0.88
0.20	0.00	0.60
0.28	0.0016	0.408
0.30	0.002	0.36
0.40	0.07	0.20
0.50	0.14	0.11
0.60	0.22	0.04
0.66	0.27	0.00

Capillary pressure is set to zero.

Gravity constant g=9.80665 m s^{-2}

DERIVED QUANTITIES

The following quantities are derived from the dataset.

Mobility ratio M and saturation at the front

From a Buckley-Leverett calculation the saturation at the front is 0.46, which is used to determine the position of the front from the reservoir simulator results. Also, the average saturation behind the front is 0.573 which, according to the recommendation of Craig [9], gives a mobility ratio M=1.46, and a=1/M=0.69.

Dimensionless rates

From Eq.17: $q_D=23.5$

From Eq.18: $q_D^c=4.6$

Step saturation change

The step saturation change S for piston-like displacement used in the analytical solution is given by:

$S=S_{oi}-S_{or}$

$= 0.66-0.28=0.38$

Dimensionless variables

Based on Eq.16 the following dimensionless variables are defined, all in SI-units:

Dimensionless radius r_D

$$r_D=r/h$$

Dimensionless height to front Y

$$Y = y/h$$

Dimensionless rate q_D

$$q_D=q/(2\pi h^2\Delta\varrho g\lambda_o)$$

Dimensionless time t_D

$$t_D=t\Delta\varrho g\lambda_o/(\phi Sh)$$